

Action Recognition with Domain Invariant Features of Skeleton Image

Han Chen Yifan Jiang Hanseok Ko*
School of Electrical Engineering, Korea University
145 Anam-ro, Seongbuk-gu, Seoul, South Korea
{jessicachan, yfjiang, hsko}@korea.ac.kr

Abstract

Due to the fast processing-speed and robustness it can achieve, skeleton-based action recognition has recently received the attention of the computer vision community. The recent Convolutional Neural Network (CNN)-based methods have shown commendable performance in learning spatio-temporal representations for skeleton sequence, which use skeleton image as input to a CNN. Since the CNN-based methods mainly encoding the temporal and skeleton joints simply as rows and columns, respectively, the latent correlation related to all joints may be lost caused by the 2D convolution. To solve this problem, we propose a novel CNN-based method with adversarial training for action recognition. We introduce a two-level domain adversarial learning to align the features of skeleton images from different view angles or subjects, respectively, thus further improve the generalization. We evaluated our proposed method on NTU RGB+D. It achieves competitive results compared with state-of-the-art methods and 2.4%, 1.9% accuracy gain than the baseline for cross-subject and cross-view.

1. Introduction

Human action recognition is one of the most popular research areas in computer vision, which has been widely used in surveillance systems, human-computer interaction, video understanding, etc. In the last few years, with the advance of 3D sensing techniques such as Microsoft Kinect, human action recognition utilizing 3D skeleton data arises a great deal of attention. Compared to RGB, skeleton data has the advantage of being computationally efficient due to smaller data sizes. Moreover, skeleton data are more robust to illumination, clustered background, and camera motion.

With the increasing development and impressive performance of deep learning methods in most of the pattern

recognition tasks, deep learning methods using Convolutional Neural Network (CNN), Recurrent Neural Network (RNN) and Graph Convolutional Network (GCN) with skeleton data also come into view. Some studies utilized the end-to-end learning based on RNN with Long-Short Term Memory (LSTM) to learn the temporal dynamics [1, 2, 3, 4, 5, 6, 7]. Even if these methods present comparative results in skeleton-based action recognition due to their capability of modeling temporal sequence, they ignored the strong dependencies among the skeleton joints in the spatial domain. Recent studies have shown the superiority of CNN over RNN for this task [8, 9, 10, 11, 12, 13, 14]. Most of the CNN-based methods encoded the trajectories of skeleton joints into image space. They benefited from CNN's admirable ability to extract high-level spatial-temporal features of skeleton images. However, during convolutional operation, only the neighboring joints within the convolutional kernel will be considered. In other words, some latent correlation that is related to all joints may be neglected. Inspired by the fact that human 3D-skeleton is naturally a topological graph, the GCN has been adopted in the action recognition task recently for the reason that its effectiveness of representing the graph structure data [15, 16, 17, 18, 19]. Most recent GCN-based methods assume that the thorough skeleton joints are available while not considering the incomplete case, which is common in real scenarios.

Unsupervised domain adaptation (UDA) aims to transfer a model learned on a labeled source domain to an unlabeled target domain. Recently, deep UDA has aroused great attention in image classification [20, 21, 22, 23, 24, 25] and semantic segmentation [26, 27, 28, 29]. There are several strategies proposed to gain better UDA performance. Some studies utilize maximum mean discrepancy (MMD) [30] to minimize differences between feature distributions [21, 31, 32], its effect is limited by whether the distributions follow Gaussian distribution. Another strategy is self-training, which utilizes predictions from an ensemble model as pseudo-labels for unlabeled data to train the current model [33, 28, 34]. There is increasing interest in the use of adversarial training to achieve UDA [35, 25, 29, 36, 37].

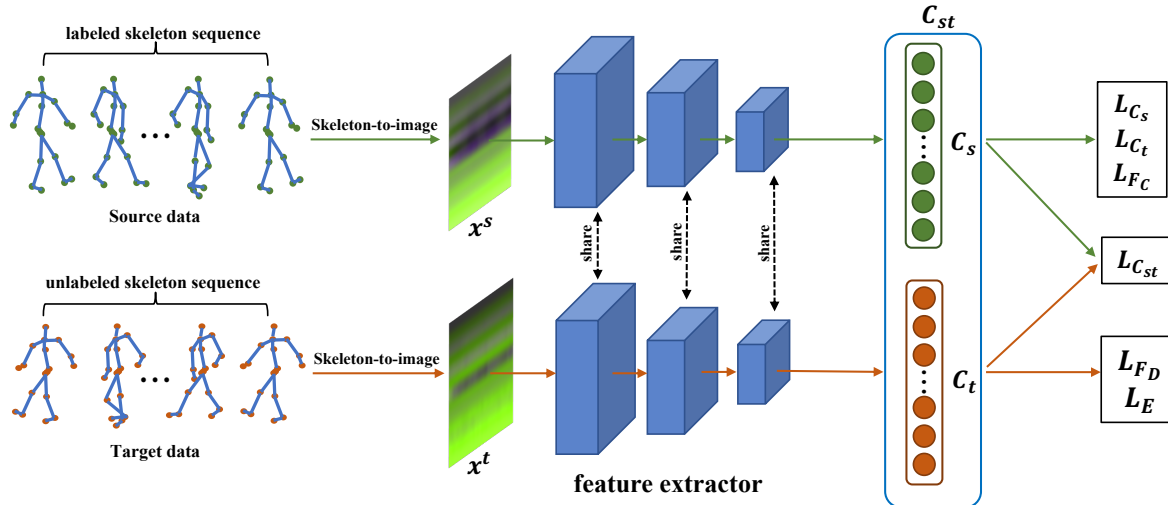


Figure 1. An illustration of our proposed method architecture. We define the two domain inputs as source and target, where the source represents the labeled skeleton sequence of one view (or subject). The target represents the unlabeled skeleton sequence of another view (or subject). Our network includes a feature extractor, source task classifier C_s , target task classifier C_t and a domain classifier C_{st} . Weights of all layers of feature extractor are shared for both source and target domain, and the C_{st} shares neurons with C_s and C_t . The green and orange colors illustrate the data flow of source and target, respectively. The right column shows a series of loss functions, please refer to the Section 2.2 and 2.3 for the definition details.

This approach reduces the shift by forcing the features from different domains to fool the discriminator, thus leading to features from different domains exhibiting a similar distribution. For the task of action recognition, a universal and reliable system needs to be robust to different viewpoints while observing an action sequence. Therefore, several works have been proposed to utilize UDA to exploit disentangled universal representations from data of different views [38, 39, 14, 40, 41]. However, very few studies have attempted deep UDA for skeleton data, so this is still an open, challenging problem.

Motivated by the success of the adversarial-training based UDA technique in image classification, we believe that CNN-based human action recognition from 3D skeleton data can benefit from this strategy. In this work, we propose a novel scheme to improve the CNN-based action recognition network, which utilizes adversarial training to drive the learned features of the intermediate network to be view-invariant or subject-invariant. We first encode the 3D skeleton sequence into a skeleton image, which served CNN for classification. For the labeled source skeleton images, the CNN network will take them as input and be trained in a supervised manner to have the classification ability. We assume that features of skeleton images from different views or subjects have a latent correlation. We propose utilizing the class-level and domain-level adversarial losses to enhance the invariant feature learning of skeleton images from different views or subjects.

The remainder of this paper is organized as follows. In

Section 2, we first give an overview of our proposed network and introduce three process phases. Experimental results and analysis are presented in Section 3. Finally, we conclude this work in Section 4.

2. Proposed Method

This section presents our proposed method for action recognition with domain invariant features of skeleton images. In Figure 1, we present an overview of our proposed method. It consists of three phases: skeleton image representation, two domain task classifiers and high-level feature learning with a two-level domain adversarial strategy. Here, we define the two domains as source and target. The source means the labeled skeleton data of one view angle (or subject), the target represents the unlabeled skeleton data of another view angle (or subject). The aim is to utilize the unlabeled data to learn the domain invariant features of skeleton data, thus further improving the network’s generalization ability to other views or subjects.

2.1. Skeleton image representation

As shown in Figure 1, given a skeleton sequence, we first map it to 2D image space. The X, Y, and Z coordinate information of the skeleton will be mapped to each channel of an RGB image, respectively. The rows represent different skeleton joints in the skeleton image, while the columns serve as the different frames. For the scenario where multiple subjects appear simultaneously, we concatenate the skeleton images of different subjects along the joint

dimension. To suit the fixed input size of the 2D CNN, we further resize the skeleton image to a standard size. We denote the generated skeleton images from source and target as x^s and x^t , respectively.

2.2. Learning of source and target task classifiers

The proposed feature extractor follows the structure of ResNet-50 [42] but excluding the last fully connected layer of it. There are two parallel classifiers C_s , C_t for source skeleton image and target skeleton image respectively, each of them is based on a single fully connected layer followed by the softmax operation and contains K neurons which equal to the class number of the actions. Besides, there is another domain classifier C_{st} , it shares neurons with C_s and C_t .

The task classifier C_s for the source domain is trained with the following cross-entropy loss over the labeled source skeleton images,

$$L_{C_s} = -\frac{1}{N_s} \sum_{i=1}^{N_s} y_i^s \log(p^s(x_i^s)) \quad (1)$$

where N_s represents the number of source skeleton images, y_i^s is the category label of the skeleton image, $p^s(x_i^s)$ is the output predicted probability of C_s .

To train the task classifier C_t for the target domain, we utilize the labeled source skeleton image and update C_t with the following loss function,

$$L_{C_t} = -\frac{1}{N_s} \sum_{i=1}^{N_s} y_i^s \log(p^t(x_i^s)) \quad (2)$$

where $p^t(x_i^s)$ is the output predicted probability of C_t .

To distinguish between the C_s and C_t , we introduce the domain classifier C_{st} in our network. It is achieved by applying the following loss,

$$L_{C_{st}} = -\frac{1}{N_s} \sum_{i=1}^{N_s} \log\left(\sum_{k=1}^K p_k^s(x_i^s)\right) - \frac{1}{N_t} \sum_{j=1}^{N_t} \log\left(\sum_{k=1}^K p_k^t(x_j^t)\right) \quad (3)$$

where N_t represents the number of target skeleton images, $\sum_{k=1}^K p_k^s(x_i^s)$ and $\sum_{k=1}^K p_k^t(x_j^t)$ represent the probabilities of classifying the input skeleton image as the source and target respectively. By updating the C_{st} with loss (3), when we send the skeleton image of source domain to the network, the first term will be approximate to 1 and larger than the second term. Similarly, when we send the skeleton image of the target domain to the network, the second term will approximate to 1 and be larger than the first term. In this way, the C_s and C_t will be distinguishable.

2.3. Learning of feature extractor through the two-level domain adversarial training

We utilize domain-level and class-level adversarial losses to align the feature distribution of source skeleton image and target skeleton image, respectively. These two losses are both achieved by adversarial learning, and through the two-level learning, the feature extractor tends to learn the domain invariant feature.

We define the domain-level adversarial loss over the unlabeled target skeleton image as follows,

$$L_{F_D} = -\frac{1}{N_t} \sum_{j=1}^{N_t} \log\left(\sum_{k=1}^K p_k^s(x_j^t)\right) - \frac{1}{N_t} \sum_{j=1}^{N_t} \log\left(\sum_{k=1}^K p_k^t(x_j^t)\right) \quad (4)$$

where N_t represents the number of source skeleton images, different from the loss (3) used to update the classifier, the domain-level adversarial loss here is used to confuse the learned features of two domains to the maximum extent. That is, to make the feature extractor learn the common representation of source skeleton image and target skeleton image so that the classifier cannot distinguish which domain the feature map comes from.

The class-level adversarial loss is calculated over the labeled source skeleton image because we can get access to the class label of the source data. It is defined as the following function,

$$L_{F_C} = -\frac{1}{N_s} \sum_{i=1}^{N_s} y_i^s \log(p^s(x_i^s)) - \frac{1}{N_s} \sum_{i=1}^{N_s} y_i^s \log(p^t(x_i^s)) \quad (5)$$

To further improve the representation ability of the feature extractor, we also introduce the entropy minimization [43] to the updating stage. The principle is to encourage the low-density separation between classes by minimizing the entropy of the class-conditional distribution of target data [44]. In our work, the loss is described in the follows,

$$L_E = -\frac{1}{N_t} \sum_{j=1}^{N_t} \sum_{k=1}^K p_k^s(x_j^t) \log(p_k^s(x_j^t)) - \frac{1}{N_t} \sum_{j=1}^{N_t} \sum_{k=1}^K p_k^t(x_j^t) \log(p_k^t(x_j^t)) \quad (6)$$

2.4. Overall training objective function

We define the overall loss function of our proposed approach as follows,

$$\min_{C_s, C_t} (L_{C_s} + L_{C_t} + L_{C_{st}}) \quad (7)$$

$$\min_F (L_{F_C} + \alpha(L_{F_D} + L_E))$$

The first three terms are used to update the classifier layer, and the last three terms are for updating the feature extractor F . The α is the hyperparameter to balance different losses.

3. Experiments

We evaluate the performance of our proposed method on the NTU RGB+D dataset [45], we compare our proposed method with other state-of-the-art skeleton-based methods reported on the same dataset.

3.1. Experimental settings

Dataset. The NTU RGB+D dataset is the largest skeleton-based human action recognition dataset to date, captured with a Microsoft Kinect V2. It contains 60 action classes ranging from daily, health-related to two-person interactive actions with a total of 56,880 sequences. The skeleton data are composed of 25 joints. The actions are recorded at the same time by three cameras set in different view angles and performed by 40 different subjects. We follow the two standard evaluation setups for this dataset: Cross-Subject (CS) and Cross-View (CV), and take the training set and the test set as two different domain. Each skeleton image is resized to 224×224 . We take the training set of the CS or CV setups as labeled source training data. As our method needs the unlabeled target data for training, so we randomly take 30% of the original test set as the target training data and the left 70% as our target test set.

Implementation details. We use PyTorch for implementation. All parameters are updated by the SGD optimizer. We set the batch size as 32 and the initial learning rate as 0.01. We follow the annealing strategy to update the learning rate. The hyperparameter α is updated by $\alpha = \frac{2}{1 + \exp(-\gamma \times p)} - 1$, where p is the progress of the training epochs normalized to the range of 0 to 1, and γ is a constant equals to 10. The structure of our network basically follows ResNet-50 [42]. We change the last fully connected layer of the ResNet-50 to a total of $2 \times$ class number neurons to construct the two task classifiers for the source domain and target domain. The other layers are treated as the feature extractor.

3.2. Experimental results

Comparison with state-of-the-art. In Table 1 we compare our proposed method with state-of-the-art skeleton-based methods on the NTU RGB+D dataset. The top-1 accuracy is chosen as the evaluation metric. The first group of methods are RNN-based methods, the second group of methods takes the CNN as the backbone, and the last group reports the results of GCN methods. The quantitative results show that our proposed method outperforms all previous RNN based and CNN-based methods in both cross-subject and

Method	CS	CV
GCA-LSTM [6]	76.1	84.0
STA-LSTM [7]	73.4	81.2
Clips + CNN + Concatenation [8]	77.1	81.1
Clips + CNN + MTLN [8]	79.6	84.8
Res-TCN [13]	74.3	83.1
Enhanced skeleton visualization [14]	76.0	82.6
F2CSkeleton [10]	79.6	84.6
TSA [11]	72.2	81.7
TSRJI [12]	73.3	80.3
A ² GNN [15]	72.7	82.8
STGCK [18]	74.9	86.3
PA-GCN [19]	80.4	82.7
Our baseline (ResNet-50) on 70% test	78.6	83.9
Our baseline (ResNet-50) on test	78.8	84.1
Ours	81.0	85.8

Table 1. Comparison with state-of-the-art methods for action recognition on NTU RGB+D dataset in accuracy (%).

cross-view scenarios, demonstrating that the learned feature representation is invariant to changes of view angle and subject. Our method also achieves comparable results with GCN-based methods, of which the computational complexity is typically over 15 GFLOPs for one skeleton sequence. Conversely, our method is composed of the lightweight CNN and appropriate losses. It just requires 3.8 GFLOPs for every skeleton sample. Please note that all state-of-the-art methods compared here are tested on the complete test set. However, our method achieves the domain invariant features learning by introducing data from the unlabeled target domain (30% of the test set) for training. In order to achieve a fair comparison, we tested the effect of our baseline on 70% test data and complete test data, respectively. We found that the difference between them is not significant, and the performance of the latter is even better than the former. Therefore, we can also prove that the results of the proposed method tested on 70% test are comparable to the results of the SOTA methods above.

Effect of different loss terms in our method. To demonstrate the effectiveness of our proposed method and different loss terms, we evaluate different variants of our method. All experiments are conducted on Cross-subject and Cross-view on NTU RGB+D dataset. First, we train ResNet-50 with the source skeleton image using the cross-entropy classification loss in a supervised manner and then test the trained network with the target test data (denoted as our baseline (ResNet-50)). Next, exclude the domain-level adversarial loss of our proposed method (denoted as Ours w/o L_{FD}). Similarly, we exclude the entropy minimization loss (denoted as Ours w/o L_E) to examine its necessity. As shown in Table 2, our proposed method improves the baseline accuracy by 2.4% and 1.9% for cross-subject

Method	CS (%)	CV (%)
Our baseline (ResNet-50)	78.6	83.9
Ours w/o L_{FD}	80.6	84.9
Ours w/o L_E	79.8	85.2
Ours	81.0	85.8

Table 2. Ablation study of different loss terms in our proposed method.

and cross-view, respectively. This demonstrates the effectiveness of our proposed scheme for learning the domain invariant feature of the skeleton image. We also observe that in the cross-subject setup, there is a more significant accuracy drop when excluding L_E than L_{FD} , which represents that the entropy minimization contributes more than the domain-level adversarial loss in cross-subject. On the contrary, in the cross-view setup, the domain-level adversarial loss shows more importance than the other.

Analysis of classification confusion matrix. To further reveal the performance of our proposed method on each class, we show the confusion matrix on NTU RGB+D in Figure 2. The diagonal represents the correct classification for each action class. The non-diagonals show the misclassification results across different action classes. As shown in Figure 2, compared with the baseline, the confusion matrix of our proposed method is cleaner than baseline both in cross-subject and cross-view setups. In other words, our method can achieve more accurate prediction and fewer misclassification than baseline. The success of our method can be attributed to our two-level adversarial learning scheme, through which our network can learn the domain invariant features of skeleton images from different views or subjects. Besides, there is still some confusion in our results. For example, the action 11-reading tends to be classified as action 29-play with a phone. We attribute it to the fact that these two actions occur in similar motions and are prone to be confused when only using the skeleton images. In the future, our work will consider the RGB data as complementary information to the skeleton images so that to solve the above misclassification situation.

4. Conclusions

In this paper, we proposed a novel action recognition network based on CNN and leverages unlabeled skeleton data from multiple views or subjects to learn view-invariant or subject-invariant feature representations of skeleton images. Our network learned the robust features for action recognition tasks by two-level domain adversarial learning strategy and entropy minimization. We trained our network on the NTU RGB+D dataset and demonstrated the effectiveness of our method on both cross-subject and cross-view setups. Experimental results showed that our proposed net-

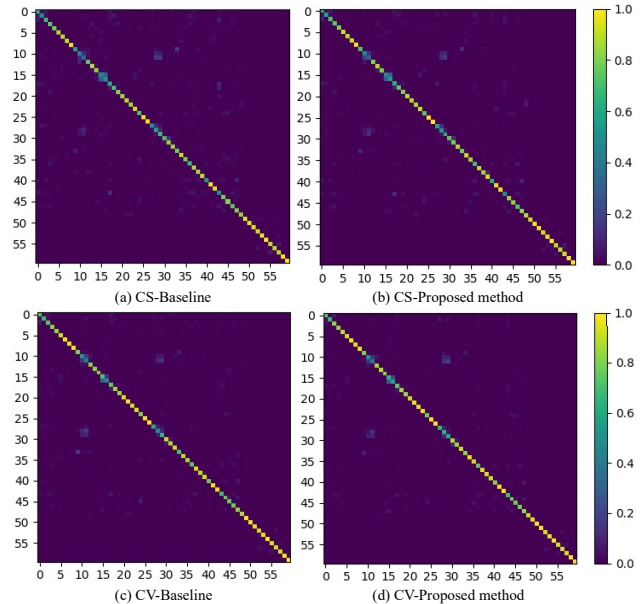


Figure 2. Confusion matrix of the baseline (ResNet-50) and our proposed method on NTU RGB+D dataset across cross-subject (CS) and cross-view (CV) evaluation setups. X-axis (True class) and Y-axis (Predicted class) are associated through the indices of action classes.

work outperforms baseline and state-of-the-art CNN-based methods. In the future, we will explore the fusion of the RGB modality into our network.

5. Acknowledgement

This work was supported by the Major Project of the Korea Institute of Civil Engineering and Building Technology (KICT) [grant number number 20210397-001].

References

- [1] Inwoong Lee, Doyoung Kim, Seoungyoon Kang, and Sanghoon Lee. Ensemble deep learning for skeleton-based action recognition using temporal sliding lstm networks. In *Proceedings of the IEEE international conference on computer vision*, pages 1012–1020, 2017. 1
- [2] Chenyang Si, Wentao Chen, Wei Wang, Liang Wang, and Tieniu Tan. An attention enhanced graph convolutional lstm network for skeleton-based action recognition. In *Proceedings of the IEEE/CVF Conference on Computer Vision and Pattern Recognition*, pages 1227–1236, 2019. 1
- [3] Yun Han, Sheng-Luen Chung, Qiang Xiao, Wei You Lin, and Shun-Feng Su. Global spatio-temporal attention for action recognition based on 3d human skeleton data. *IEEE Access*, 8:88604–88616, 2020. 1
- [4] Aichun Zhu, Qianyu Wu, Ran Cui, Tian Wang, Wenlong Hang, Gang Hua, and Hichem Snoussi. Exploring a rich

- spatial-temporal dependent relational model for skeleton-based action recognition by bidirectional lstm-cnn. *Neurocomputing*, 414:90–100, 2020. 1
- [5] Wing Ng, Mingyang Zhang, and Ting Wang. Multi-localized sensitive autoencoder-attention-lstm for skeleton-based action recognition. *IEEE Transactions on Multimedia*, 2021. 1
- [6] Jun Liu, Gang Wang, Ling-Yu Duan, Kamila Abdiyeva, and Alex C Kot. Skeleton-based human action recognition with global context-aware attention lstm networks. *IEEE Transactions on Image Processing*, 27(4):1586–1599, 2017. 1, 4
- [7] Sijie Song, Cuiling Lan, Junliang Xing, Wenjun Zeng, and Jiaying Liu. An end-to-end spatio-temporal attention model for human action recognition from skeleton data. In *Proceedings of the AAAI conference on artificial intelligence*, volume 31, 2017. 1, 4
- [8] Qihong Ke, Mohammed Bennamoun, Senjian An, Ferdous Sohel, and Farid Boussaid. A new representation of skeleton sequences for 3d action recognition. In *Proceedings of the IEEE conference on computer vision and pattern recognition*, pages 3288–3297, 2017. 1, 4
- [9] Chao Li, Qiaoyong Zhong, Di Xie, and Shiliang Pu. Skeleton-based action recognition with convolutional neural networks. In *2017 IEEE International Conference on Multimedia & Expo Workshops (ICMEW)*, pages 597–600. IEEE, 2017. 1
- [10] Thao Minh Le, Nakamasa Inoue, and Koichi Shinoda. A fine-to-coarse convolutional neural network for 3d human action recognition. *arXiv preprint arXiv:1805.11790*, 2018. 1, 4
- [11] Carlos Caetano, Jessica Sena, François Brémond, Jeferson A Dos Santos, and William Robson Schwartz. Skelemotion: A new representation of skeleton joint sequences based on motion information for 3d action recognition. In *2019 16th IEEE International Conference on Advanced Video and Signal Based Surveillance (AVSS)*, pages 1–8. IEEE, 2019. 1, 4
- [12] Carlos Caetano, François Brémond, and William Robson Schwartz. Skeleton image representation for 3d action recognition based on tree structure and reference joints. In *2019 32nd SIBGRAPI conference on graphics, patterns and images (SIBGRAPI)*, pages 16–23. IEEE, 2019. 1, 4
- [13] Tae Soo Kim and Austin Reiter. Interpretable 3d human action analysis with temporal convolutional networks. In *2017 IEEE conference on computer vision and pattern recognition workshops (CVPRW)*, pages 1623–1631. IEEE, 2017. 1, 4
- [14] Mengyuan Liu, Hong Liu, and Chen Chen. Enhanced skeleton visualization for view invariant human action recognition. *Pattern Recognition*, 68:346–362, 2017. 1, 2, 4
- [15] Chaolong Li, Zhen Cui, Wenming Zheng, Chunyan Xu, Rongrong Ji, and Jian Yang. Action-attending graphic neural network. *IEEE Transactions on Image Processing*, 27(7):3657–3670, 2018. 1, 4
- [16] Xiang Gao, Wei Hu, Jiaxiang Tang, Jiaying Liu, and Zongming Guo. Optimized skeleton-based action recognition via sparsified graph regression. In *Proceedings of the 27th ACM International Conference on Multimedia*, pages 601–610, 2019. 1
- [17] Yongsang Yoon, Jongmin Yu, and Moongu Jeon. Predictively encoded graph convolutional network for noise-robust skeleton-based action recognition. *Applied Intelligence*, pages 1–15, 2021. 1
- [18] C Li, Z Cui, W Zheng, C Xu, and J Yang. Spatio-temporal graph convolution for skeleton based action recognition (2018). *arXiv preprint arXiv:1802.09834*. 1, 4
- [19] Yang Qin, Lingfei Mo, Chenyang Li, and Jiayi Luo. Skeleton-based action recognition by part-aware graph convolutional networks. *The visual computer*, 36(3):621–631, 2020. 1, 4
- [20] Yaroslav Ganin, Evgeniya Ustinova, Hana Ajakan, Pascal Germain, Hugo Larochelle, François Laviolette, Mario Marchand, and Victor Lempitsky. Domain-adversarial training of neural networks. *The journal of machine learning research*, 17(1):2096–2030, 2016. 1
- [21] Muhammad Ghifary, W Bastiaan Kleijn, and Mengjie Zhang. Domain adaptive neural networks for object recognition. In *Pacific Rim international conference on artificial intelligence*, pages 898–904. Springer, 2014. 1
- [22] Mingsheng Long, Yue Cao, Jianmin Wang, and Michael Jordan. Learning transferable features with deep adaptation networks. In *International conference on machine learning*, pages 97–105. PMLR, 2015. 1
- [23] Mingsheng Long, Han Zhu, Jianmin Wang, and Michael I Jordan. Deep transfer learning with joint adaptation networks. In *International conference on machine learning*, pages 2208–2217. PMLR, 2017. 1
- [24] Baochen Sun and Kate Saenko. Deep coral: Correlation alignment for deep domain adaptation. In *European conference on computer vision*, pages 443–450. Springer, 2016. 1
- [25] Eric Tzeng, Judy Hoffman, Kate Saenko, and Trevor Darrell. Adversarial discriminative domain adaptation. In *Proceedings of the IEEE conference on computer vision and pattern recognition*, pages 7167–7176, 2017. 1
- [26] Haoshuo Huang, Qixing Huang, and Philipp Krahenbuhl. Domain transfer through deep activation matching. In *Proceedings of the European Conference on Computer Vision (ECCV)*, pages 590–605, 2018. 1
- [27] Yang Zhang, Philip David, and Boqing Gong. Curriculum domain adaptation for semantic segmentation of urban scenes. In *Proceedings of the IEEE international conference on computer vision*, pages 2020–2030, 2017. 1
- [28] Yang Zou, Zhiding Yu, BVK Kumar, and Jinsong Wang. Unsupervised domain adaptation for semantic segmentation via class-balanced self-training. In *Proceedings of the European conference on computer vision (ECCV)*, pages 289–305, 2018. 1

- [29] Fei Pan, Inkyu Shin, Francois Rameau, Seokju Lee, and In So Kweon. Unsupervised intra-domain adaptation for semantic segmentation through self-supervision. In *Proceedings of the IEEE/CVF Conference on Computer Vision and Pattern Recognition*, pages 3764–3773, 2020. [1](#)
- [30] Arthur Gretton, Karsten M Borgwardt, Malte J Rasch, Bernhard Schölkopf, and Alexander Smola. A kernel two-sample test. *The Journal of Machine Learning Research*, 13(1):723–773, 2012. [1](#)
- [31] Hongliang Yan, Yukang Ding, Peihua Li, Qilong Wang, Yong Xu, and Wangmeng Zuo. Mind the class weight bias: Weighted maximum mean discrepancy for unsupervised domain adaptation. In *Proceedings of the IEEE Conference on Computer Vision and Pattern Recognition*, pages 2272–2281, 2017. [1](#)
- [32] Philip Haeusser, Thomas Frerix, Alexander Mordvintsev, and Daniel Cremers. Associative domain adaptation. In *Proceedings of the IEEE International Conference on Computer Vision*, pages 2765–2773, 2017. [1](#)
- [33] Hongmin Li, Doina Caragea, Cornelia Caragea, and Nic Herndon. Disaster response aided by tweet classification with a domain adaptation approach. *Journal of Contingencies and Crisis Management*, 26(1):16–27, 2018. [1](#)
- [34] Teo Spadotto, Marco Toldo, Umberto Michieli, and Pietro Zanuttigh. Unsupervised domain adaptation with multiple domain discriminators and adaptive self-training. In *2020 25th International Conference on Pattern Recognition (ICPR)*, pages 2845–2852. IEEE, 2021. [1](#)
- [35] Tuan-Hung Vu, Himalaya Jain, Maxime Bucher, Matthieu Cord, and Patrick Pérez. Advent: Adversarial entropy minimization for domain adaptation in semantic segmentation. In *Proceedings of the IEEE conference on computer vision and pattern recognition*, pages 2517–2526, 2019. [1](#)
- [36] Jinguang Jiang, Yifei Ji, Ximei Wang, Yufeng Liu, Jianmin Wang, and Mingsheng Long. Regressive domain adaptation for unsupervised keypoint detection. In *Proceedings of the IEEE/CVF Conference on Computer Vision and Pattern Recognition*, pages 6780–6789, 2021. [1](#)
- [37] Ibrahim Batuhan Akkaya, Fazil Altinel, and Ugur Halici. Self-training guided adversarial domain adaptation for thermal imagery. In *Proceedings of the IEEE/CVF Conference on Computer Vision and Pattern Recognition*, pages 4322–4331, 2021. [1](#)
- [38] Min-Hung Chen, Zsolt Kira, Ghassan AlRegib, Jaekwon Yoo, Ruxin Chen, and Jian Zheng. Temporal attentive alignment for large-scale video domain adaptation. In *Proceedings of the IEEE/CVF International Conference on Computer Vision*, pages 6321–6330, 2019. [2](#)
- [39] Arshad Jamal, Vinay P Namboodiri, Dipti Deodhare, and KS Venkatesh. Deep domain adaptation in action space. In *BMVC*, volume 2, page 5, 2018. [2](#)
- [40] Junnan Li, Yongkang Wong, Qi Zhao, and Mohan S Kankanhalli. Unsupervised learning of view-invariant action representations. *arXiv preprint arXiv:1809.01844*, 2018. [2](#)
- [41] Gunnar A Sigurdsson, Abhinav Gupta, Cordelia Schmid, Ali Farhadi, and Karteek Alahari. Actor and observer: Joint modeling of first and third-person videos. In *Proceedings of the IEEE Conference on Computer Vision and Pattern Recognition*, pages 7396–7404, 2018. [2](#)
- [42] Kaiming He, Xiangyu Zhang, Shaoqing Ren, and Jian Sun. Deep residual learning for image recognition. In *Proceedings of the IEEE conference on computer vision and pattern recognition*, pages 770–778, 2016. [3](#), [4](#)
- [43] Kuniaki Saito, Donghyun Kim, Stan Sclaroff, Trevor Darrell, and Kate Saenko. Semi-supervised domain adaptation via minimax entropy. In *Proceedings of the IEEE/CVF International Conference on Computer Vision*, pages 8050–8058, 2019. [3](#)
- [44] Yves Grandvalet, Yoshua Bengio, et al. Semi-supervised learning by entropy minimization. *CAP*, 367:281–296, 2005. [3](#)
- [45] Amir Shahroudy, Jun Liu, Tian-Tsong Ng, and Gang Wang. Ntu rgb+d: A large scale dataset for 3d human activity analysis. In *Proceedings of the IEEE conference on computer vision and pattern recognition*, pages 1010–1019, 2016. [4](#)